

Figure S1. Profiling cell surface expression of Fc γ RI and Fc γ RII on THP-1 cells. Anti-Fc γ RI (CD64) clone 10.1 (BD Biosciences), anti-Fc γ RII (CD32) clone IV.3, and anti-Fc γ RIII (CD16) clone 3G8 were used to label the empty vector transfected CHO cells (CHO-EV) and THP-1 cells.

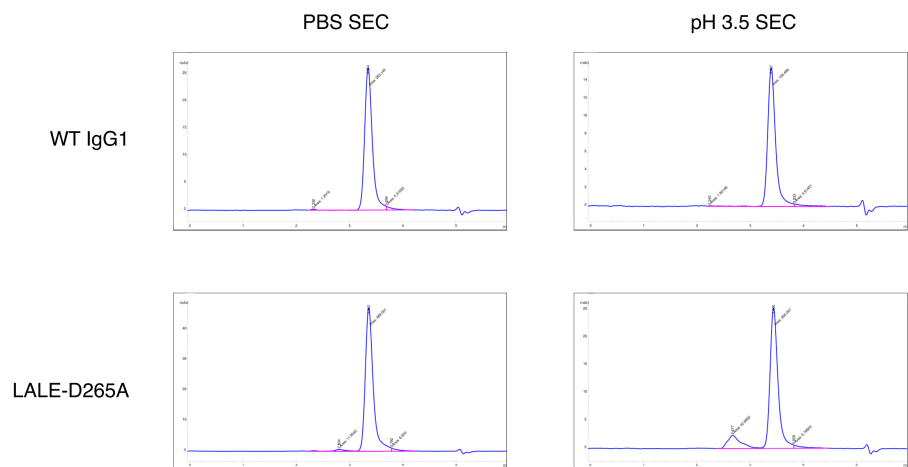


Figure S2. Representative SEC profiles for WT IgG1 and LALE-D265A variants under standard (PBS) and pH 3.5 conditions.

Table S1. Octet BLI characterization of the binding of the lower hinge panel to Cy CD3 $\delta\epsilon$.

| IgG1 Hinge Mutations | Cy CD3 $\delta\epsilon$ Fc (RU) |
|----------------------|---------------------------------|
| WT IgG1 | 0.47 |
| L234A/L235A (LALA) | 0.55 |
| L234F/L235E (LFLE) | 0.55 |
| L234A/L235E (LALE) | 0.56 |

| | |
|----------------------------|------|
| L235A/G237A (LAGA1) | 0.53 |
| L234A/G237A (LAGA2) | 0.52 |
| L234A/L235A/G237A (LALAGA) | 0.55 |
| L234A/L235K (LALK) | 0.53 |
| L234F/L235K (LFLK) | 0.56 |
| L234E/L235K (LELK) | 0.59 |
| WT IgG2 | 0.51 |

Table S2. Octet BLI characterization of the binding of the lower hinge CH2 mutation combination panel to ProA, Hu CD3 $\delta\epsilon$, and Cy CD3 $\delta\epsilon$.

| IgG1 Hinge x CH2 Mutations | Octet Kinetics | | |
|----------------------------|----------------|---------------------------------|---------------------------------|
| | ProA (RU) | Hu CD3 $\delta\epsilon$ Fc (RU) | Cy CD3 $\delta\epsilon$ Fc (RU) |
| N/A | 4.6 | 0.52 | 0.45 |
| LALA | 4.9 | 0.59 | 0.54 |
| LALA-D265A | 4.7 | 0.51 | 0.59 |
| LALA-S267K | 4.9 | 0.45 | 0.57 |
| LALA-H268Q | 4.8 | 0.51 | 0.59 |
| LALA-D270A | 5.0 | 0.43 | 0.57 |
| LALA-L309A | 4.8 | 0.45 | 0.59 |
| LALA-L309V | 4.6 | 0.45 | 0.60 |
| LALA-K322A | 4.8 | 0.44 | 0.55 |
| LALA-A327G | 4.7 | 0.54 | 0.57 |
| LALA-L328A | 4.9 | 0.59 | 0.59 |
| LALA-P329A | 4.9 | 0.56 | 0.61 |
| LALA-P329G | 4.8 | 0.53 | 0.60 |
| LALA-Y296F | 4.9 | 0.47 | 0.59 |
| LALA-A330S | 5.0 | 0.56 | 0.59 |
| LALA-P331S | 5.0 | 0.57 | 0.61 |
| LALA-A330S/P331S | 4.7 | 0.53 | 0.58 |
| LALE | 5.1 | 0.56 | 0.50 |
| LALE-D265A | 4.8 | 0.59 | 0.63 |
| LALE -S267K | 4.8 | 0.55 | 0.49 |
| LALE-H268Q | 5.1 | 0.52 | 0.48 |
| LALE-D270A | 4.9 | 0.52 | 0.48 |
| LALE-L309A | 4.7 | 0.53 | 0.49 |
| LALE-L309V | 0.0 | 0.56 | 0.51 |
| LALE-K322A | 4.6 | 0.53 | 0.51 |
| LALE-L328A | 4.7 | 0.55 | 0.49 |
| LALE-P329G | 5.0 | 0.55 | 0.49 |
| LALE-P329A | 4.9 | 0.57 | 0.52 |
| LALE-A330S | 5.1 | 0.54 | 0.48 |
| LALE-P331S | 5.1 | 0.55 | 0.47 |
| LALE-A330S/P331S | 5.0 | 0.58 | 0.51 |
| LALAGA-P329G | 5.0 | 0.56 | 0.43 |